marine drugs

MDPI

Article

Marine Microalga *Tisochrysis lutea* F&M-M36 Modulates Gut Microbiota and Intestinal Cholesterol Transport Gene Expression in Association with Selected Early-Stage Metabolic Alterations Under High-Fat Feeding

Elisabetta Bigagli [1,†], Niccolò Meriggi [2,†], Mario D'Ambrosio [1,3], Natascia Biondi [4], Liliana Rodolfi [4,5], Alberto Niccolai [4], Gianluca Bartolucci [1], Marta Menicatti [1], Carlotta de Filippo [2,*] and Cristina Luceri [1,*]

1 Department of NEUROFARBA, University of Florence, Viale Pieraccini 6, 50139 Florence, Italy; elisabetta.bigagli@unifi.it (E.B.); dambrosio.mario@mayo.edu (M.D.); gianluca.bartolucci@unifi.it (G.B.); marta.menicatti@unifi.it (M.M.)
2 Institute of Agricultural Biology and Biotechnology (IBBA), National Research Council (CNR), 56124 Pisa, Italy; niccolo.meriggi@cnr.it
3 Enteric Neuroscience Program, Department of Medicine, Section of Gastroenterology and Hepatology, Mayo Clinic, Rochester, MN 55905, USA
4 Department of Agriculture, Food, Environment and Forestry (DAGRI), University of Florence, Piazzale delle Cascine 18, 50144 Florence, Italy; natascia.biondi@unifi.it (N.B.); liliana.rodolfi@unifi.it (L.R.)
5 Fotosintetica & Microbiologica S.r.l., Via di Santo Spirito 14, 50125 Florence, Italy
* Correspondence: carlotta.defilippo@cnr.it (C.d.F.); cristina.luceri@unifi.it (C.L.)
† These authors contributed equally to this work as co-first authors.

Abstract

Modulation of the gut microbiota represents a promising approach to counteract diet-induced metabolic alterations, with microalgae emerging as potential interventions. Building on our previous in vivo evidence that dietary supplementation with the marine microalga *Tisochrysis lutea* F&M-M36 (*T. lutea*) positively modulates selected metabolic alterations under high-fat feeding, the present study aimed to identify potential associations between these metabolic changes and coordinated modifications of the gut microbiota. Animals were fed normal-fat (NF), high-fat (HF), or HF supplemented with 5% *T. lutea* (HFTiso) diets for three months. Gut microbial profiles were analyzed by 16S rRNA sequencing and correlated with plasma lipids, glucose, blood pressure, fecal lipid excretion, and adiponectin levels. *T. lutea* supplementation was associated with significant modulation of selected metabolic parameters and coherent alterations in gut microbial communities. Multivariate analyses revealed treatment-dependent clustering of metabolic profiles, with HFTiso forming an intermediate group between HF and NF diets. Beta-diversity analyses showed marked treatment-specific shifts, while alpha-diversity remained stable. Linear discriminant analysis identified 31 discriminative genera, with the HFTiso group enriched in taxa associated with fermentative metabolism and lipid-related metabolic pathways including *Anaerotruncus*, *Marvinbryantia*, and *Eubacterium coprostanoligenes*, while the HF group was linked to *Clostridium sensu stricto 1* and *Terrisporobacter*. Positive correlations between HFTiso-associated taxa and adiponectin levels were consistent with microbiota-associated metabolic signatures. In parallel, *T. lutea* supplementation was associated with downregulation of colonic Niemann-Pick C1-like 1 (NPC1L1) mRNA expression, a key mediator of intestinal cholesterol uptake. The bioactivity of *T. lutea* likely reflects its content of polyunsaturated fatty acids, oleic acid, phytosterols, and fucoxanthin; however, whether these components act synergistically or whether specific bioactive compounds are primarily responsible remains to be clarified. Together, these findings indicate that *T. lutea* supplementation is associated with coordinated changes in gut microbiota composition and

Check for updates

Academic Editor: Nisansala Liyanage

Received: 1 December 2025
Revised: 16 February 2026
Accepted: 19 February 2026
Published: 21 February 2026

Copyright: © 2026 by the authors. Licensee MDPI, Basel, Switzerland. This article is an open access article distributed under the terms and conditions of the Creative Commons Attribution (CC BY) license.

transcriptional modulation of the intestinal cholesterol transporter NPC1L1 in the context of selected early-stage metabolic alterations under high-fat feeding. While direct extrapolation to humans remains limited, these results suggest potential translational relevance of *T. lutea* as a nutraceutical approach targeting early-stage metabolic dysregulation. Future studies will be required to determine the mechanistic contribution of individual bioactive components and to assess whether microbiota- and gene expression-associated changes play a causal role in mediating the observed metabolic outcomes, thereby informing the rational development of *T. lutea*-derived interventions.

Keywords: microalgae; *Tisochrysis lutea*; microbiota; lipid metabolism; cardiovascular diseases; cardiometabolic risk; nutraceutics

1. Introduction

Cardiometabolic health is increasingly threatened by interconnected risk factors, including obesity, insulin resistance, dyslipidemia, and hypertension, which jointly predispose individuals to cardiovascular diseases (CVD), type 2 diabetes mellitus (T2DM), and related metabolic disorders [1]. According to the Global Burden of Disease Study, suboptimal dietary patterns accounted for approximately 1.55 million CVD-related deaths in 2019 [2]. Enhancing cardiometabolic health thus represents a major public health priority, aiming to prevent the onset and progression of CVD.

Emerging evidence highlights the gut microbiota as a central regulator of cardiometabolic health influencing host metabolism through short-chain fatty acid (SCFA) production, bile acid regulation, and modulation of systemic inflammation [3]. Conversely, dysbiosis, characterized by reduced microbial diversity and decreased abundance of SCFA-producing taxa, has been associated with insulin resistance, dyslipidemia, and chronic low-grade inflammation [4]. In this context, restoring eubiosis through diet or bioactive compounds supplementation represents a promising strategy to improve metabolic outcomes and CV risk profiles [5].

Microalgae have recently gained attention as sustainable sources of bioactive molecules capable of beneficially modulating the gut microbiota and improving cardio-metabolic health [6–9].

Recent studies have demonstrated that the well-known microalgae *Spirulina platensis* and *Chlorella pyrenoidosa* exert anti-obesity, anti-diabetic, anti-hypertensive, lipid-lowering, and anti-inflammatory effects through modulation of the gut microbiota. Their bioactive compounds, particularly polysaccharides and polyunsaturated fatty acids, enhance microbial diversity, decrease the Firmicutes/Bacteroidetes ratio, and increase beneficial taxa such as *Prevotella*, *Alloprevotella*, and *Lactobacillaceae* while reducing harmful bacteria like *Turicibacter* and *Clostridium_XlVa*. These changes are associated with increased SCFA production, reduced gut permeability, and restoration of bile acid and trimethylamine pathways [6–9], supporting a microbiome-mediated mechanism underlying the metabolic benefits of microalgal supplementation.

Among marine microalgae, *Tisochrysis lutea* (*T. lutea*) stands out for its high content of bioactive compounds, including ω-3 fatty acids (mainly docosahexaenoic acid (DHA)), polyphenols, and carotenoids such as fucoxanthin, all known for their anti-inflammatory and anti-dyslipidemic properties [10,11]. Although *T. lutea* is currently used primarily in aquaculture and has not yet been approved for human consumption [12], we previously demonstrated that high dietary addition of *T. lutea* F&M-M36 was well tolerated and unexpectedly improved lipid metabolism even under iso-caloric feeding conditions [13]. Mayer et al. also found that dietary supplementation with *T. lutea* ameliorated lipid

and glucose metabolism and reduced inflammation in rats fed a high-fat, high-fructose diet, likely due to the synergistic interaction among DHA, fucoxanthin, phytosterols, and fibers [14]. We also showed that the *T. lutea* F&M-M36 methanolic extract exerts anti-inflammatory effects in vitro by inhibiting the COX-2/PGE_2 pathway and the NLRP3 inflammasome/microRNA-223 axis with effects more evident than those of fucoxanthin alone [11].

More recently, we demonstrated that *T. lutea* F&M-M36 improves multiple high-fat induced cardiometabolic alterations, reducing plasma triglycerides and glucose, increasing fecal lipid excretion and adiponectin, and modulating key metabolic proteins such as β_3-adrenergic receptor, uncoupling protein 1, and glucagon-like peptide-1 receptor. Transcriptomic analyses also revealed activation of energy metabolism pathways and suppression of inflammatory and autophagy-related genes, suggesting a multifaceted mechanism of action [15].

Building on our previous in vivo evidence, the present study was designed as a microbiota-oriented extension of earlier metabolic observations [15]. Specifically, we investigated the impact of *T. lutea* supplementation on gut microbiota composition and its associations with selected metabolic and vascular readouts previously shown to be affected in this experimental model [15]. In addition, we explored whether *T. lutea* supplementation is associated with transcriptional modulation of intestinal cholesterol transporter Niemann–Pick C1-like 1 (NPC1L1), a key mediator of intestinal cholesterol uptake. Exploring these host–microbiota associations was intended to identify transcriptional and microbial patterns potentially contributing to the metabolic effects previously observed with *T. lutea* supplementation, thereby generating hypothesis for future mechanistic studies on *T. lutea*-derived interventions targeting pathways relevant to cardiometabolic risk.

2. Results

2.1. Characterization of the Microalgal Biomass

The biochemical composition, fucoxanthin and phenolic compounds composition of *T. lutea* F&M-M36 have been previously reported [11,13] and is summarized here solely to provide compositional context for the biological outcomes investigated in the present study. For reference, the macromolecular composition of dried microalgal biomass had 4.3% carbohydrates, 15.1% lipids, 42.4% proteins, 18.2% fibers, and 13.1% ashes (Supplementary Table S1) [13]. The fatty acid composition of *T. lutea* revealed a balanced profile of ω-3, ω-6, and ω-9 polyunsaturated fatty acids. The ω-3 fraction was dominated by α-linolenic acid (ALA, C18:3n-3; 10.6%) and docosahexaenoic acid (DHA, C22:6n-3; 6.7%), with additional contributions from eicosatrienoic acid (C20:3n-3; 2.3%). The ω-6 fraction included linoleic acid (LA, C18:2n-6; 7.5%) and γ-linolenic acid (C18:3n-6; 0.3%). Oleic acid (C18:1n-9; 19.3%) represented the major ω-9 fatty acid. Overall, the biomass exhibited a high ω-3 content relative to ω-6, with substantial DHA levels characteristic of *T. lutea*, alongside a significant proportion of ω-9 fatty acids (Supplementary Table S2). As previously reported [11], we characterized fucoxanthin and phenolic compounds in a methanolic extract of *T. lutea* F&M-M36, obtaining 4.7 mg/g DW of fucoxanthin and 6.22 ± 0.05 mg GAE/g DW of total soluble phenolics. The phenolic profile was dominated by simple C6 and C6–C1 structures, including hydroxybenzoic acid and gallic acid derivatives, as well as some aromatic amino acids [11].

2.2. Host Metabolic and Bacterial Diversity Shift After Dietary Treatment

Differences in metabolic profiles of the six metabolic variables revealed clear separation among groups along the first two principal components as displayed in PCA (Figure 1b). PC1 explained 50.2% of the variance, while PC2 accounted for 20%, together representing

70.2% of the total variability, reflecting the presence of a strong underlying gradient in metabolic variations. Samples from the HF group clustered predominantly on the positive side of PC1, whereas NF samples were positioned toward the negative axis. The HFTiso group showed an intermediate distribution, partially overlapping with both HF and NF clusters but forming a distinct grouping. Adonis PERMANOVA analysis confirmed that treatment significantly explained variation in the metabolic dataset ($R^2 = 0.522$, $F = 7.65$, $p < 0.001$) (Figure 1b). Thus, more than half of the variance in metabolic parameters was attributable to differences among HF, HFTiso, and NF groups.

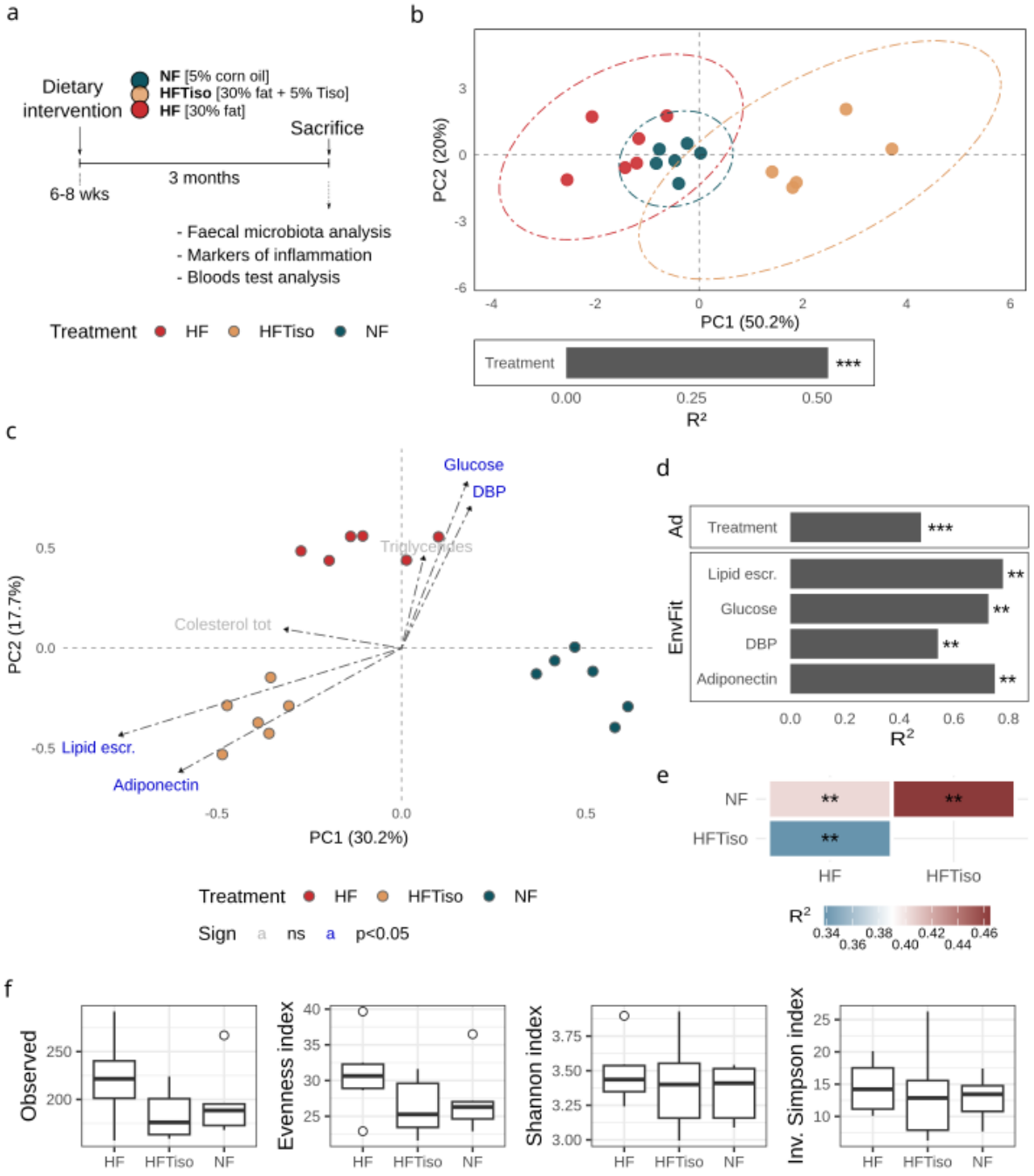

Figure 1. Differences in metabolic and bacterial profiles among treatment groups. (**a**) Schematic representation of experimental design reporting the dietary intervention. (**b**) PCA based on Euclidean

distance highlights the sample distribution according to the metabolic profiles represented by total cholesterol, glucose, diastolic blood pressure (DBP), lipid excretion, and adiponectin levels. Samples are colored according to the treatment group (HF, HFTiso, NF), and group dispersion was visualized by confidence ellipses. The proportion of variance explained (R^2 from adonis PERMANOVA) and the significance level were reported in the barplot below the ordinational plot (***, $p < 0.001$). (**c**) PCA based on Hellinger distance reports the sample distribution based on differences in bacterial ASVs transformed relative abundances at the end of experiment. Significant vectors (FDR < 0.05), obtained from environmental fitting analysis (envfit), were plotted as arrows within the ordination diagram. (**d**) Barplots report the amount of variance explained by significant factors tested, i.e., treatment (Ad: R^2 from adonis PERMANOVA) (***, $p < 0.001$) and vector tested in the environmental fitting analysis (EnvFit: R^2 from *envfit* function). Significance annotations for each factor are reported using asterisks (**, p-adj < 0.01). (**e**) Heatmaps report the R^2 values (color gradient) from pairwise adonis PERMANOVA with significance annotations for each treatment group comparison (**, p-adj < 0.01). (**f**) Boxplots report the alpha-diversity metrics among treatment groups. Group comparisons are evaluated using the Wilkoxon test (FDR adjustment method).

Dietary treatment significantly impacted on bacterial diversity and composition. The adonis PERMANOVA based on Bray–Curtis distances revealed that treatment explained around 47.9% of the variance in bacterial community composition ($R^2 = 0.479$, $F = 6.91$, $p < 0.001$ in Supplementary Table S3). Pairwise PERMANOVA confirmed that all groups were significantly different from each other, with R^2 values ranging from 0.34 (HF vs. HFTiso) to 0.46 (HFTiso vs. NF) (adjusted $p < 0.01$) (Figure 1e). The RDA ordination (Hellinger distance) showed clear samples clustering according to dietary treatment (Figure 1c). The first two axes explained a substantial proportion of community variability (30.2% and 17.7% for first and second axis respectively), capturing the main variance differences between HF, HFTiso, and NF samples. Environmental fitting analysis (*envfit*) identified several host metabolic parameters as significantly correlated with community variation after FDR correction (Supplementary Table S4). Specifically, glucose levels ($R^2 = 0.727$, $p = 0.002$), DBP ($R^2 = 0.541$, $p = 0.006$), lipid excretion ($R^2 = 0.780$, $p = 0.002$), and adiponectin levels ($R^2 = 0.750$, $p = 0.002$) were strongly associated with bacterial diversity variations in multidimensional space, while triglycerides and total cholesterol were not significant (Figure 1c,d). Vectors corresponding to significant variables were oriented consistently with the separation of treatment groups in the ordination biplot (Figure 1c), indicating that changes in host lipid-related readouts and adiponectin levels were significantly associated with differences in bacterial community. In detail, increased levels of lipid excretion and adiponectin positively covaried with the HFTiso-related cluster, while an increase in glucose levels and DBP positively covaried with the HF-related cluster (Figure 1c).

Bacterial richness and diversity (alpha diversity) did not significantly differ between groups (Figure 1f). The total number of ASVs (observed richness) were comparable across groups, with no significant differences detected after pairwise comparisons (all p-adj ≥ 0.36) as well as for Shannon diversity index (all p-adj = 1.0), Inverse Simpson index (all p-adj ≥ 0.88) and Pielou's evenness (all p-adj ≥ 0.88) (Supplementary Table S5). The results indicate that dietary treatment did not significantly affect within-sample bacterial diversity. Therefore, while beta-diversity analyses revealed strong treatment-dependent clustering (see above sections), alpha diversity remained stable across groups.

2.3. T. lutea Reshapes Gut Microbiota and Related Metabolic Interactions

LDA-based differentially abundant analysis selected 70 bacterial features after the Kruskal–Wallis test, reduced to 40 after a subsequent Wilcoxon test, then the LDA threshold (LDA ≥ 2.5) selected 31 significantly discriminative bacterial features (Supplementary Table S6). Among the bacterial genera selected by LDA, Clostridium

sensu stricto 1 and Terrisporobacter were significantly associated with the HF diet, while genera Hoeflea, Erysipelatoclostridium, Anaerotruncus, Acetatifactor, Corynebacterium, [Eubacterium] coprostanoligenes and brachy groups, *Gordonibacter*, *Marvinbryantia*, and *Intestinimonas* were significantly associated with the HFTiso treatment (Figure 2a). Therefore, *Bifidobacterium*, *Butyrivibrio*, *Papillibacter*, *[Eubacterium] ruminantium group*, *Acetatifactor* and broader clades such as Firmicutes were significantly linked to the baseline dietary intervention, i.e., NF treatment (Figure 2a).

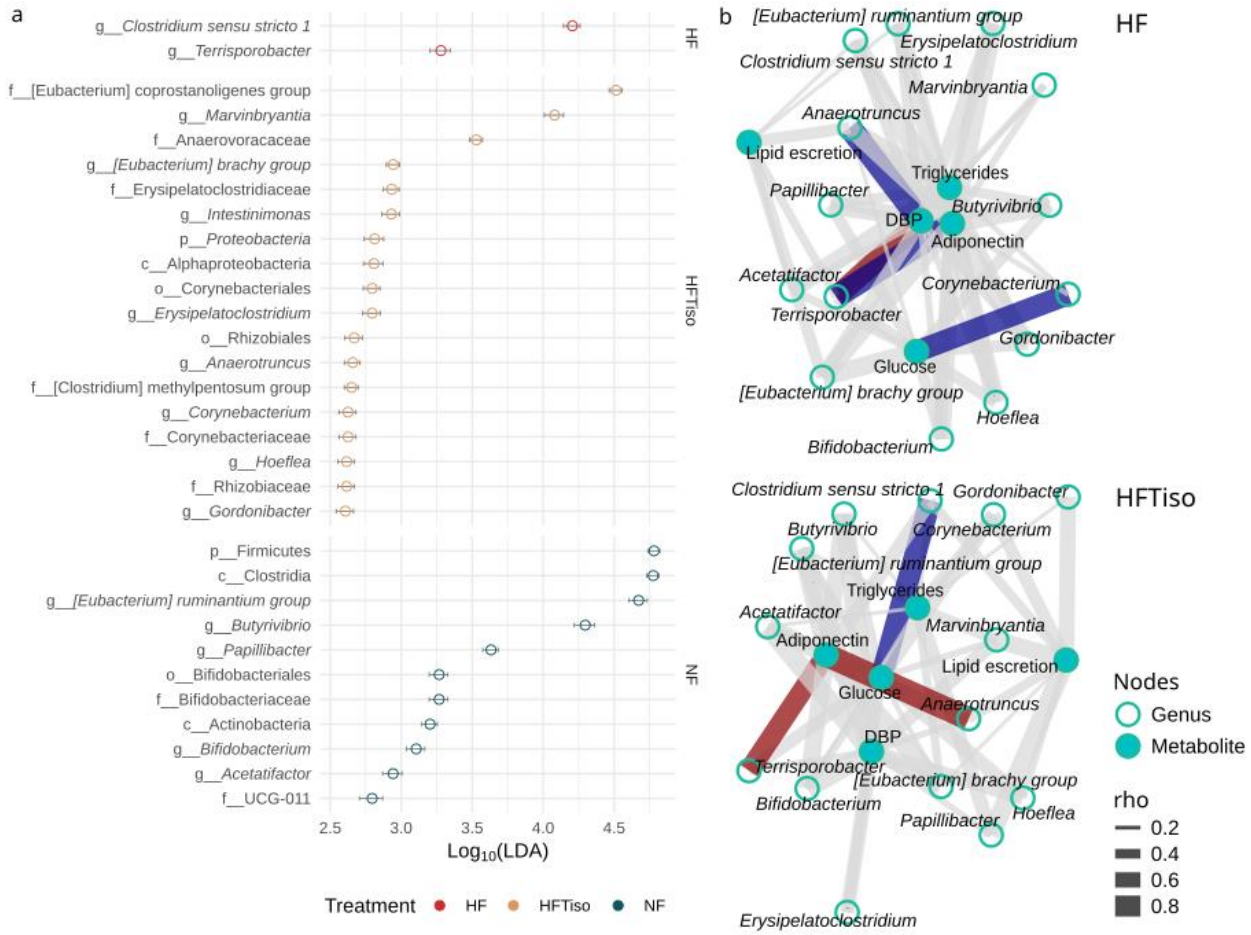

Figure 2. Bacterial discriminant analysis and metabolic correlation. (**a**) Differentially abundant taxa identified by LDA effect size analysis (LDA > 2.5). Bars indicate LDA mean ± lower and upper confidence intervals for taxa discriminating between HF, HFTiso, and NF groups (color scheme in the legend). (**b**) Correlation networks constructed using the Kamada–Kawai layout of HF and HFTiso datasets, between gut bacterial genera (LDA selected) and host metabolic variables. Nodes represent metabolites (filled light blue circles) or microbial genera (empty light blue circles). Edges represent Spearman correlations with rho $\geq$ 0.2 only and edge color indicates correlation direction and significance (red = positive significant, blue = negative significant, grey = not significant).

Overall, the LDA approach revealed distinct genus-level microbial signatures across the experimental groups, demonstrating compositional differences primarily driven by members of *Firmicutes*, *Actinobacteria*, and *Proteobacteria* phyla. These significantly discriminative genera were subsequently selected for correlation analyses with host metabolic variables, allowing the identification of microbiota–metabolite associations that may underline treatment-specific physiological responses.

Spearman correlation analysis was performed to investigate potential associations between significantly discriminative bacterial genera, identified through LDA analysis, and host metabolic variables among HF and HFTiso. The resulting networks revealed distinct

patterns of microbiota–metabolite interactions that significantly change among the HF and HFTiso groups.

The HF correlation network highlighted a strong positive association between *Terrisporobacter* and diastolic blood pressure (DBP, rho = 0.83, $p = 0.0416$), whereas *Terrisporobacter* displayed a negative correlation with adiponectin levels (rho = −0.89, $p = 0.0188$), and *Anaerotruncus* was also negatively correlated with DBP (rho = −0.89, $p = 0.0188$) (HF on Figure 2b). In addition, *Corynebacterium* showed a significant negative correlation with glucose concentrations (rho = −0.83, $p = 0.0416$) (Figure 2b). The dietary integration with *T. lutea* (HFTiso in Figure 2b) significantly switches the pattern displayed by correlation network analysis. In particular, *Anaerotruncus* and *Terrisporobacter* were positively correlated with adiponectin (rho = 0.83, $p = 0.0416$) (HFTiso in Figure 2b).

2.4. Effects of T. lutea F&M-M36 on Gene Expression in the Colon and SCFAs Plasmatic Levels

T. lutea had a significant effect on NPC1L1 mRNA expression (ANOVA, $p = 0.0046$). Post hoc analysis (Dunn test with FDR correction) revealed that the HFTiso treatment significantly reduced NPC1L1 mRNA expression compared with both HF (adjusted $p = 0.0088$) and NF (adjusted $p = 0.0103$). No significant difference was detected between the HF and NF groups (adjusted $p = 0.7869$). Conversely, *T. lutea* did not significantly affect the expression of occludin (ANOVA, $p = 0.576$) or TJP-1 (Kruskal–Wallis test, $p = 0.142$) (Figure 3).

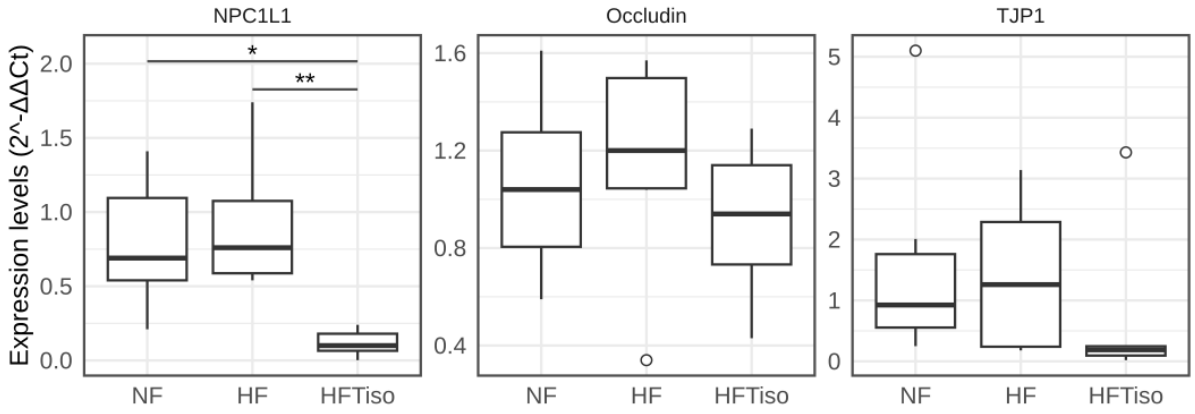

Figure 3. Gene expression of TJP1, Occludin, and NPC1L1. Boxplots display the gene expression levels ($2^{-\Delta\Delta Ct}$) across treatment groups (NF, HF, HFTiso). Significant post hoc differences for NPC1L1 were assessed using Dunn's test with FDR correction and reported using asterisks (**, $p < 0.01$; *, $p < 0.05$).

The plasmatic levels of short-chain fatty acids (SCFAs) were compared across the three experimental groups (HF, HFTiso, and NF). Overall, no statistically significant differences in total or individual SCFAs concentrations were detected among the HF, HFTiso, and NF groups after correction for multiple comparisons (all adjusted p-values > 0.05: Supplementary Table S7). Nonetheless, the variations in concentrations between groups revealed consistent trends across several metabolites. Total SCFAs showed higher mean concentrations in the HFTiso group compared with both HF and NF groups. A similar pattern was observed for acetic acid, hexanoic, propionic and butyric acids which displayed the highest mean levels in HFTiso compared to the other groups (Supplementary Figure S1). Although these differences did not reach statistical significance, the observed trends suggest a potential modulation of SCFAs production profiles across dietary treatments, warranting further investigation in larger cohorts or complementary experimental settings.

3. Discussion

The present work was conceived as a microbiota-oriented extension of our earlier metabolic observations [15] rather than as comprehensive cardiometabolic phenotyping. In this context, it provides new insights into microbiota-associated patterns consistent with previously observed positive effects of *T. lutea* F&M-M36 in selected early-stage metabolic alterations under high-fat feeding. Our previous findings showed that *T. lutea* improves lipid profiles, blood pressure, and glucose metabolism by enhancing energy metabolism and suppressing inflammatory pathways [15]. In line with this evidence, the current multivariate analyses revealed treatment-dependent clustering of metabolic profiles with the *T. lutea*-supplemented group forming a distinct cluster, with partial overlap with both the NF and HF groups. This pattern is expected, as the HF model was intentionally designed to reproduce a pre-metabolic syndrome-like condition rather than overt disease, a stage considered particularly suitable for dietary interventions [16].

Treatment-associated shifts in selected metabolic readouts were accompanied by coherent alterations in gut microbiota composition. β-diversity analysis revealed treatment-dependent clustering, whereas α-diversity remained unchanged, indicating that *T. lutea* primarily reshapes community structure rather than overall microbial richness.

In line with these findings, LDA-based differential abundance analysis identified distinct bacterial signatures across dietary groups. The *T. lutea*-supplemented group was enriched in taxa belonging to the Alphaproteobacteria and Rhizobiaceae families, including *Hoeflea* and *Gordonibacter*, as well as several Clostridiales-related genera such as *Erysipelatoclostridium*, *Anaerotruncus*, and *Marvinbryantia*. The bacterial species *Eubacterium coprostanoligenes* is of particular interest due to its reported ability to convert cholesterol into coprostanol, a non-absorbable sterol, thereby reducing intestinal cholesterol absorption and circulating cholesterol levels [17]. Previous studies have associated *E. coprostanoligenes* abundance with improved cardiometabolic traits, including under metformin treatment [18] and reduced thrombotic risk [19]. While causality cannot be established in the present model, these observations provide biological plausibility for the contribution of *T. lutea*-associated taxa to intestinal lipid homeostasis. The genus *Marvinbryantia*, belonging to the Lachnospiraceae family, has been associated with SCFA-related pathways, particularly acetate and butyrate, which are commonly linked to intestinal homeostasis and anti-inflammatory processes [20]. Although circulating SCFAs did not differ significantly between groups, *T. lutea* supplementation was associated with consistent trends toward higher mean levels of total SCFAs and key metabolites such as acetate, propionate, and butyrate. These trends are biologically coherent with the observed microbial shifts, but they should be interpreted cautiously as the lack of statistical significance and the exploratory nature of the correlation analyses preclude functional inference. In addition, in observational studies, higher abundance of *Marvinbryantia* has been inversely associated with insulin resistance or T2DM [21], while members of the Anaerovoracaceae family have been reported to correlate negatively with serum leptin levels in animal models [22].

Conversely, the HF dietary signature was characterized by genera, such as *Clostridium sensu stricto* 1 and *Terrisporobacter*, that have been linked to lipid and amino acid fermentation and, in the context of high-fat feeding, to altered bile acid profiles and inflammation [23–26].

Terrisporobacter has been associated with unfavorable cardiometabolic traits in human studies [24–26]; however, such associations may be strongly context-dependent and influenced by diet and host metabolic state. In the present study, correlation network analyses revealed diet-dependent relationships between *Terrisporobacter*, *Anaerotruncus*, and host metabolic readouts, with positive associations with adiponectin emerging in the *T. lutea*-supplemented group. Similarly, *Anaerotruncus* showed opposite correlations across

dietary groups, being negatively associated with diastolic blood pressure and positively associated with adiponectin in the *T. lutea*–supplemented group. These patterns suggest a context-dependent remodeling of host–microbiota interactions rather than fixed beneficial or detrimental roles of specific taxa.

In contrast, the NF group showed enrichment of taxa including *Butyrivibrio*, *Papillibacter*, and *Bifidobacterium*, which is consistent with a gut microbial profile associated with a low-inflammatory intestinal environment [27–29].

In line with the pre-metabolic nature of the experimental model, the absence of changes in tight junction gene expression argues against major impairment of intestinal barrier integrity. Notably, *T. lutea* supplementation significantly downregulated colonic NPC1L1 mRNA expression, a key mediator of intestinal cholesterol uptake and the pharmacological target of ezetimibe. Although NPC1L1 modulation was assessed only at the mRNA level and protein-level measurements or functional assays of cholesterol absorption were not performed, previous in vivo dietary intervention models have shown that transcriptional downregulation of intestinal NPC1L1 is associated with reduced cholesterol absorption [30]. NPC1L1 expression is also influenced by the gut microbiota, and both genetic deletion and pharmacological inhibition of NPC1L1 have been reported to reshape microbial composition in experimental models [30,31]. Accordingly, the concurrent NPC1L1 downregulation and microbiota remodeling observed in the *T. lutea*-supplemented group is consistent with coordinated host–microbiota interactions; however, no mechanistic or target-specific role can be inferred from the present data. Definitive assessment of NPC1L1 involvement will require protein-level validation, functional cholesterol absorption assays, and dedicated genetic or pharmacological approaches in future studies.

The complex biochemical profile of *T. lutea*, including ω-3 polyunsaturated fatty acids, oleic and myristic acids, phytosterols, fucoxanthin, and phenolic compounds [11,13–15], provides biological plausibility for host-driven metabolic effects that may secondarily influence host–microbiota interactions. These compounds have been reported to modulate lipid and glucose metabolism and influence energy balance in experimental models [15,32,33]. Although fucoxanthin and phenolic compounds are characterized by relatively low systemic bioavailability, they may nonetheless contribute to metabolic regulation through local intestinal actions and microbiota-associated mechanisms, together with systemically active components such as ω-3 polyunsaturated fatty acids, oleic acid, and phytosterols. In addition, docosahexaenoic acid (DHA) and oleic acid serve as precursors of oleoylethanolamide, a lipid mediator involved in the regulation of appetite, energy balance, and intestinal homeostasis [34]. However, the observational nature of the present study and the reliance on correlation-based analyses do not allow discrimination between primary microbiota-driven effects and secondary adaptations to host metabolic remodeling induced by *T. lutea* supplementation.

Several limitations should be acknowledged: (1) This study was conducted exclusively in male rats, and potential sex-specific differences in response to *T. lutea* supplementation cannot be excluded. (2) The 5% dietary dose used in rats corresponds to an estimated human-equivalent intake of approximately 45 g/day for a 70 kg adult, which exceeds typical dietary exposure; however, similar or higher inclusion levels of microalgal biomass (up to 15% of the diet) have been employed in preclinical models to investigate metabolic and microbiota-related mechanisms, supporting the use of such doses for mechanistic exploration [35]. Moreover, human intervention studies with microalgae-based supplements, such as spirulina, have reported daily intakes up to 19 g/day [36], indicating that relatively high levels of microalgal biomass can be safely administered in controlled settings. (3) Whether the bioactive components of *T. lutea* act synergistically or whether specific compounds predominantly drive the observed associations remains to be clarified

in order to guide the rational development of optimized formulations, extracts, or enriched fractions targeting pathways relevant to cardiometabolic risk while improving translational feasibility. (4) Future studies are necessary to validate the mechanistic contribution of individual components and to determine whether microbiota- and gene expression-associated changes play a causal role in mediating the metabolic effects of *T. lutea*. Despite these limitations, the present findings indicate that *T. lutea* supplementation is associated with coordinated changes in gut microbiota composition and transcriptional modulation of the intestinal cholesterol transporter NPC1L1, in the context of selected early-stage metabolic alterations under high-fat feeding. While mechanistic causality cannot be inferred, these results may contribute to guiding future studies and the development of optimized *T. lutea*-derived interventions.

4. Materials and Methods

4.1. Microalga Cultivation and Production

T. lutea F&M-M36 biomass (from the Fotosintetica & Microbiologica (F&M) S.r.l. culture collection, Florence, Italy) was produced at Archimede Ricerche S.r.l. (Camporosso, Imperia, Italy) in GWP®-II photobioreactors operating in semi-batch mode using F culture medium [37,38]. The biomass was collected by centrifugation, then frozen, freeze-dried, ground into powder, and finally stored at −20 °C until use.

4.2. Characterization of the Microalgal Biomass

The biochemical and macromolecular composition of *T. lutea* F&M-M36 reported in this section derives from previous detailed characterizations of the same strain and is included here solely to contextualize the biological outcomes investigated in the present study. These data are not presented as newly generated analytical results. Although different biomass batches were produced, the same strain (F&M-M36), cultivation system, culture medium, and downstream processing pipeline were applied, minimizing batch-to-batch variability.

The analytical methods used for compositional characterization are briefly summarized below for completeness and reproducibility, as previously reported [13]. Briefly, total protein content was calculated as N × 6.25 from elemental nitrogen using a CHNSO Analyzer (Flash EA, 1112 Series, Thermo Electron Corporation, USA) Carbohydrates were quantified according to [39], and total lipids by the method of Marsh and Weinstein [40]. Moisture content was determined following ISTISAN Report 1996/34 (Method B). Fiber content was measured according to AOAC Method 985.29. Fatty acid composition was evaluated according to the official food analysis method of the Italian Ministry of Health (ISTISAN Report 1996/34). Briefly, total lipids were extracted from dried biomass using a chloroform–methanol mixture. The extracted lipids were subjected to acid-catalyzed transesterification to obtain fatty acid methyl esters (FAMEs). FAMEs were analyzed by gas chromatography–mass spectrometry (GC–MS) using an Agilent GC–MS system equipped with a capillary column suitable for fatty acid separation. Helium was used as carrier gas at constant flow. The injector and detector temperatures, as well as the oven temperature program, were set according to previously validated conditions [41]. Fatty acids were identified by comparison of retention times and mass spectra with those of a Supelco® 37-component FAME standard mix and reference libraries. Phenolics were isolated by liquid–liquid partitioning to remove pigments and analyzed by HPLC-DAD (UV detection at 280 and 350 nm). Fucoxanthin was quantified by HPLC using a C30 reverse-phase column and an MTBE/methanol gradient with internal-standard calibration according to a modification [11] of the method by Kim et al. [42].

4.3. Experimental Design and Animal Treatments

All procedures were conducted in accordance with the European Union regulations on the care and use of laboratory animals (OJ of ECL 358/1, 18 December 1986) and the Italian regulations on the protection of animals used for experimental and other scientific purposes (DM 116/1992). The study was approved by the Italian Ministry for Scientific Research (Authorization ID 1137/2015; approval date: 28 October 2015).

The detailed experimental procedures have been previously reported [15] and are briefly summarized here. Male Sprague Dawley rats (Nossan S.r.l., Milan, Italy), aged 6–8 weeks, were divided into three experimental groups, rats fed the AIN-76 diet (NF 5% fat, rats fed a high-fat diet (HF 30% fat), and rats fed a HF diet supplemented with 5% *T. lutea* F&M-M36 biomass (HFTiso), and fed for 3 months. Diets were adjusted to account for macronutrient content of *T. lutea* F&M-M36 biomass (Supplementary Table S8), and all animals had ad libitum access to food and water under a 12 h light/dark cycle.

For the purposes of this study, a subgroup of N = 6 animals per group was selected from the original cohort (N = 8) to characterize gut microbial composition and explore correlations with host metabolic parameters. This approach allowed mechanistic insights into the effects of *T. lutea* supplementation on the gut microbiota and cholesterol absorption while remaining consistent with the previously reported metabolic outcomes.

4.4. Blood Biochemistry, Blood Pressure, and Fecal Lipid Analysis

At the end of the study, blood was collected for biochemical analyses. Blood pressure was measured non-invasively using a computerized tail-cuff system (Visitech BP-2000 Series II Blood Pressure Analysis System, Apex, NC, USA), and plasma lipids, glucose, and atherogenic index were determined using standard the Reflotron® Plus system (Roche Diagnostics GmbH, Mannheim, Germany). Fecal lipid content was assessed by chloroform–methanol extraction [43].

4.5. Sequencing and Amplicon Sequence Variants Inference

Fecal samples from all animals were stored at −80 °C until processing. DNA was extracted using the DNeasy PowerLyzer PowerSoil Kit (Qiagen, Hilden, Germany) according to the manufacturer's instructions. Libraries targeting the V3-V4 region of the 16S rRNA gene were prepared using primer pairs 341F (5′-CCTACGGGNGGCWGCAG-3′) and 805R (5′-GACTACNVGGGTWTCTAATCC-3′) and sequenced on the Illumina MiSeq platform in paired-end mode (PE300). Primer pairs were removed by using cutadapt v4.2 [44]. Amplicon sequence variants (ASVs) were inferred from raw reads using the DADA2 pipeline v1.26 [45]. Taxonomic assignment was carried out with the DECIPHER package v2.30 [46] against the most recent release of the SILVA small-subunit reference database (SSU v138, http://www2.decipher.codes/Downloads.html, access on 5 August 2024). DADA2 pipeline and downstream statistical analysis were performed in the R environment v4.3.1 [47].

4.6. Metabolic and Bacterial Statistical Analysis

To minimize bias, the zero-abundance ASVs were removed and sequences assigned to Archaea, Chloroplast, and Mitochondria were filtered out, resulting in a final dataset comprising 1993 ASVs with a total of 3,122,843 reads (median reads per sample: 44,531.5).

Beta-diversity analyses were carried out, after removing taxa present in only one sample within the dataset (also referred to singleton), and after normalization counts to relative abundances. Multidimensional analyses were performed by using Bray–Curtis dissimilarities, calculated using the "vegan" package v2.7.1 [48], and differences between treatment groups were inspected using permutational multivariate analysis of variance

(adonis PERMANOVA) of "vegan" package v2.7.1, setting 1000 as number of permutations. The explained variance was visualized through redundancy analysis (RDA) with Hellinger-transformed data, followed by environmental fitting analysis performed using *envfit()* function of "vegan" package v2.7.1, based on metabolic parameters from [15], then false discovery rate (FDR) correction was applied to adjust *p*-values. To reduce potential biases arising from differences in scale, all variables were standardized (mean-centered and scaled to unit variance) prior to analysis. Principal Component Analysis (PCA) was performed on the scaled data to reduce dimensionality and visualize sample distribution based on metabolic parameters. To further resolve group-specific differences, pairwise adonis PERMANOVA tests were performed by using "pairwiseAdonis" package v0.4.1, setting 1000 numbers of permutations and adjusting *p*-values using the FDR correction method [49].

To test for significant differences in multivariate metabolic profiles between treatment groups, adonis PERMANOVA was conducted on a Euclidean distance matrix with 1000 permutations, by using *adonis2* function of the "vegan" package v2.7.1.

Alpha-diversity was calculated using the "phyloseq" package v1.46 [50]. For each sample, Observed richness (number of ASVs), Shannon diversity index, Inverse Simpson index, and Pielou's evenness (calculated as Shannon/log (Observed)) were calculated. Group differences in alpha diversity metrics were assessed using pairwise Wilcoxon rank-sum tests (FDR adjusted *p*-value).

LDA-based microbial differential abundance analysis was performed using the "MicrobiotaProcess" package v1.14.1 [51], setting a $p \leq 0.05$ as a significant threshold for Kruskal–Wallis test and pairwise Wilcoxon rank-sum tests with FDR correction method. Taxa that met both criteria were subsequently subjected to LDA effect size estimation, with a discriminative threshold of LDA ≥ 2.5.

To explore associations between microbial genera and host metabolic parameters within the HF and HFTiso datasets, a correlation analysis was performed. Relative abundances were computed for each genus. To address the compositional nature of the data, abundances were transformed using a centered log-ratio (CLR) transformation after adding a pseudocount of 1×10^{-6}, while metabolic variables were standardized using z-score normalization to prevent bias due to differing scales and the relative constraints of compositional data. The correlation analysis was performed on the genera significantly selected by LDA (FDR ≤ 0.05 and LDA ≥ 2.5). Spearman correlation coefficients were computed between CLR-transformed genus abundances and scaled metabolic variables, then for each pair, correlation coefficients (rho) and associated *p*-values were calculated using the rcorr() function of "Hmisc" package v5.2.3 [52]. Correlations were classified as positive or negative, and significance was assigned using a *p*-value threshold of 0.05. Correlation networks were constructed using "igraph" package v2.1.4 and visualized with "ggraph" package v2.2.2 for correlations with rho ≥ 0.2 only [53,54].

4.7. Gene Expression Analysis

Total RNA was extracted using TRIzol reagent (Invitrogen, Carlsbad, CA, USA). First-strand cDNA was synthesized using the RevertAid RT Kit (Thermo Scientific, Waltham, MA, USA), according to the manufacturer's instructions.

Quantitative real-time PCR (qRT-PCR) assays were performed with the Rotor-Gene® QPCR System (Qiagen, Hilden, Germany) using the SsoAdvanced Universal SYBR Green Supermix (Bio-Rad, Hercules, CA, USA). Primers were designed based on the mouse GenBank sequences for TJP, Occludin and Niemann-Pick C1-like 1 (NPC1L1). The amplification protocol consisted of an initial heat activation at 95 °C for 30 s, followed by 35 cycles of

denaturation at 95 °C for 15 s and annealing/extension at 60 °C for 30 s. The relative mRNA expression levels were normalized to β-Actin and calculated using the $2^{-\Delta\Delta Ct}$ method [15].

For each gene, statistical testing procedures were selected automatically based on data distribution and variance structure, i.e., normality within each treatment group was assessed using the Shapiro–Wilk test, and homogeneity of variance was evaluated using Levene's test. When both assumptions were met, parametric analysis of variance (ANOVA) was applied; otherwise, a non-parametric Kruskal–Wallis test was performed. If a significant effect on gene expression levels was depicted, a post hoc pairwise comparison was performed using Dunn's test with multiple-comparison correction (FDR adjust method).

4.8. Evaluation of Plasma SCFAs by Gas Chromatography–Mass Spectrometry (GC–MS) Analysis

In this study, the term SCFAs refers to the classical short-chain fatty acids (acetic, propionic, butyric, isobutyric, isovaleric, and valeric acids) as well as hexanoic and iso-hexanoic acids.

Circulating SCFAs were determined by using an Agilent GC–MS system, composed of an HP 5973 single quadrupole mass spectrometer, an HP 6890 gas chromatograph, and an HP 7673 autosampler, according to described protocols [55]. Briefly, just before the analysis, each sample was thawed and the free SCFAs were extracted as follows: an aliquot of 200 µL of plasma sample was added to 10 µL of ISTD mixture ([$^2H_3$] acetic acid, [$^2H_5$] propionic acid, [$^2H_7$] isobutyric acid, [$^2H_7$] butyric acid, [$^2H_9$] isovaleric acid, [$^2H_9$] valeric acid, [$^2H_{11}$] Hexanoic acid), 200 µL of tert–butyl methyl ether and 50 µL of 6 M HCl + 0.5 M NaCl solution in a 0.5 mL centrifuge tube. Afterwards, each tube was stirred in a vortex for 5 min and centrifuged at 10,000 rpm for 5 min, and finally, the solvent layer was transferred to a vial with a microvolume insert and analyzed.

Supplementary Materials: The following supporting information can be downloaded at https://www.mdpi.com/article/10.3390/md24020086/s1, Supplementary Table S1. Nutritional profile of the microalgal biomass; Table S2. Fatty acids; Table S3. Adonis PERMANOVA performed on Bray-Curtis dissimilarities computed from relative ASVs abundances; Table S4. Environmental fitting analysis applied to the RDA ordination based on Hellinger-transformed ASVs relative abundances; Table S5. Differences in Alpha-diversity metrics across treatment groups; Table S6. Differential abundance analysis; Table S7. Variations in total and individual SCFAs among treatment groups; Figure S1. Short chain fatty acid (SCFAs) concentrations among experimental groups; Table S8. Composition of the experimental diets.

Author Contributions: Conceptualization, C.L. and E.B.; methodology, C.L., E.B., C.d.F., N.M., N.B., L.R., G.B. and M.M.; validation, C.L., E.B., C.d.F., N.M., G.B. and M.M.; formal analysis, C.d.F. and N.M.; investigation, M.D., E.B. and C.L.; resources, C.L., A.N., N.B., L.R. and C.d.F.; writing—original draft preparation, E.B.; writing—review and editing, all authors; supervision, C.L. and E.B.; funding acquisition, C.L. and C.d.F. All authors have read and agreed to the published version of the manuscript.

Funding: This research was: (i) co-funded by Ente Cassa di Risparmio Firenze grant numbers 2015.0919 and 2018.1002 and Regione Toscana (Italy) under Par-FAS 2007–2013 Projects (Centro di Competenza VALORE) and (ii) founded by the National Recovery and Resilience Plan (NRRP), Mission 4 Component 2 Investment 1.3—Call for tender No. 341 of 15 March 2022 of Italian Ministry of University and Research funded by the European Union—NextGenerationEU; Project code PE00000003, Concession Decree No. 1550 of 11 October 2022 adopted by the Italian Ministry of University and Research, Project title "ON Foods—Research and innovation network on food and nutrition Sustainability, Safety and Security—Working ON Foods".

Institutional Review Board Statement: The animal study protocol was approved by the Italian Ministry of Health-Direzione generale della sanità animale e dei farmaci veterinari (n° 1137/2017/PR, 28 October 2015).

Data Availability Statement: Raw sequences data are available at European Nucleotide Archive (ENA) under accession code PRJEB104448. All study results are presented in written form, as figures or tables in the main text or as Supplementary Material. Further information related to this study can be provided upon reasonable request to the corresponding author Cristina Luceri (cristina.luceri@unifi.it); Carlotta De Filippo (carlotta.defilippo@cnr.it).

Conflicts of Interest: *T. lutea* F&M-M36 belongs to F&M S.r.l. Culture Collection, where L.R. has a financial interest. The other authors have no conflicts of interest.

References

1. Gjermeni, E.; Fiebiger, R.; Bundalian, L.; Garten, A.; Schöneberg, T.; Le Duc, D.; Blüher, M. The impact of dietary interventions on cardiometabolic health. *Cardiovasc. Diabetol.* **2025**, *24*, 234. [CrossRef]
2. Pörschmann, T.; Meier, T.; Lorkowski, S. Cardiovascular mortality attributable to dietary risk factors in 54 countries in the WHO European Region from 1990 to 2019: An updated systematic analysis of the Global Burden of Disease Study. *Eur. J. Prev. Cardiol.* **2024**, *32*, 1553–1563. [CrossRef] [PubMed]
3. Reddy, N.; Chiwhane, A.; Acharya, S.; Kumar, S.; Parepalli, A.; Nelakuditi, M. Harnessing the power of the gut microbiome: A review of supplementation therapies for metabolic syndrome. *Cureus* **2024**, *16*, e69682. [CrossRef] [PubMed]
4. Hamjane, N.; Mechita, M.B.; Nourouti, N.G.; Barakat, A. Gut microbiota dysbiosis-associated obesity and its involvement in cardiovascular diseases and type 2 diabetes: A systematic review. *Microvasc. Res.* **2024**, *151*, 104601. [CrossRef] [PubMed]
5. Sharma, B.R.; Jaiswal, S.; Ravindra, P.V. Modulation of gut microbiota by bioactive compounds for prevention and management of type 2 diabetes. *Biomed. Pharmacother.* **2022**, *152*, 113148. [CrossRef]
6. Alves, J.L.B.; Costa, P.C.T.D.; Sales, L.C.S.; Silva Luis, C.C.; Bezerra, T.P.T.; Souza, M.L.A.; Costa, B.A.; de Souza, E.L. Shedding light on the impacts of Spirulina platensis on gut microbiota and related health benefits. *Crit. Rev. Food Sci. Nutr.* **2025**, *65*, 2062–2075. [CrossRef]
7. Li, T.T.; Huang, Z.R.; Jia, R.B.; Lv, X.C.; Zhao, C.; Liu, B. Spirulina platensis polysaccharides attenuate lipid and carbohydrate metabolism disorder in high-sucrose and high-fat diet-fed rats in association with intestinal microbiota. *Food Res. Int.* **2021**, *147*, 110530. [CrossRef]
8. Guo, W.; Zhu, S.; Li, S.; Feng, Y.; Wu, H.; Zeng, M. Microalgae polysaccharides ameliorate obesity in association with modulation of lipid metabolism and gut microbiota in high-fat-diet fed C57BL/6 mice. *Int. J. Biol. Macromol.* **2021**, *182*, 1371–1383. [CrossRef]
9. Wan, X.; Li, T.; Liu, D.; Chen, Y.; Liu, Y.; Liu, B.; Zhang, H.; Zhao, C. Effect of marine microalga Chlorella pyrenoidosa ethanol extract on lipid metabolism and gut microbiota composition in high-fat diet-fed rats. *Mar. Drugs* **2018**, *16*, 498. [CrossRef]
10. Niccolai, A.; Chini Zittelli, G.; Rodolfi, L.; Biondi, N.; Tredici, M.R. Microalgae of interest as food source: Biochemical composition and digestibility. *Algal Res.* **2019**, *42*, 101617. [CrossRef]
11. Bigagli, E.; D'Ambrosio, M.; Cinci, L.; Niccolai, A.; Biondi, N.; Rodolfi, L.; Dos Santos Nascimiento, L.B.; Tredici, M.R.; Luceri, C. A comparative in vitro evaluation of the anti-inflammatory effects of a Tisochrysis lutea extract and fucoxanthin. *Mar. Drugs* **2021**, *19*, 334. [CrossRef] [PubMed]
12. Custódio, L.; Soares, F.; Pereira, H.; Barreira, L.; Vizetto-Duarte, C.; Rodrigues, M.J.; Rauter, A.P.; Alberício, F.; Varela, J. Fatty acid composition and biological activities of Isochrysis galbana T-ISO, Tetraselmis sp. and Scenedesmus sp.: Possible application in the pharmaceutical and functional food industries. *J. Appl. Phycol.* **2014**, *26*, 151–161. [CrossRef]
13. Bigagli, E.; Cinci, L.; Niccolai, A.; Biondi, N.; Rodolfi, L.; D'Ottavio, M.; D'Ambrosio, M.; Lodovici, M.; Tredici, M.R.; Luceri, C. Preliminary data on the dietary safety, tolerability and effects on lipid metabolism of the marine microalga Tisochrysis lutea. *Algal Res.* **2018**, *34*, 244–249. [CrossRef]
14. Mayer, C.; Richard, L.; Côme, M.; Ulmann, L.; Nazih, H.; Chénais, B.; Ouguerram, K.; Mimouni, V. The marine microalga Tisochrysis lutea protects against metabolic disorders associated with metabolic syndrome and obesity. *Nutrients* **2021**, *13*, 430. [CrossRef]
15. D'Ambrosio, M.; Bigagli, E.; Cinci, L.; Gencarelli, M.; Chioccioli, S.; Biondi, N.; Rodolfi, L.; Niccolai, A.; Zambelli, F.; Laurino, A.; et al. Tisochrysis lutea F&M-M36 mitigates risk factors of metabolic syndrome and promotes visceral fat browning through β3-adrenergic receptor/UCP1 signaling. *Mar. Drugs* **2023**, *21*, 303. [CrossRef]
16. Koizumi, K.; Oku, M.; Hayashi, S.; Inujima, A.; Shibahara, N.; Chen, L.; Igarashi, Y.; Tobe, K.; Saito, S.; Kadowaki, M.; et al. Identifying pre-disease signals before metabolic syndrome in mice by dynamical network biomarkers. *Sci. Rep.* **2019**, *9*, 8767. [CrossRef]
17. Bubeck, A.M.; Urbain, P.; Horn, C.; Jung, A.S.; Ferrari, L.; Ruple, H.K.; Podlesny, D.; Zorn, S.; Laupsa-Borge, J.; Jensen, C.; et al. High-fat diet impact on intestinal cholesterol conversion by the microbiota and serum cholesterol levels. *iScience* **2023**, *26*, 107697. [CrossRef]

18. Zhou, R.; Wu, Q.; Qian, H.; Wang, L.; Liu, G.; Zhang, B.; Wu, W.; Zhang, S. Long-term metformin alters gut microbiota and serum metabolome in coronary artery disease patients after percutaneous coronary intervention to improve 5-year prognoses: A multi-omics analysis. *Rev. Cardiovasc. Med.* **2025**, *26*, 26835. [CrossRef]
19. Xi, L.; Wang, H.; Du, J.; Liu, A.; Wang, J.; Ni, Y.; Zhang, S.; Xie, W.; Liu, M.; Wang, C. Causal effect of gut microbiota on venous thromboembolism: A two-sample Mendelian randomization study. *Thromb. J.* **2024**, *22*, 106. [CrossRef]
20. He, Y.; Qin, X.; Liao, C.; Lima, R.L.S.; Hou, Q.; Lei, J.; Lai, Y.; Jiang, Q.; Wang, B.; Zhang, B. Genistein alleviates colitis by suppressing inflammation and modulating colonic Marvinbryantia formatexigens abundance and metabolites. *Curr. Res. Food Sci.* **2025**, *10*, 101016. [CrossRef]
21. Chen, Z.; Radjabzadeh, D.; Chen, L.; Kurilshikov, A.; Kavousi, M.; Ahmadizar, F.; Ikram, M.A.; Uitterlinden, A.G.; Zhernakova, A.; Fu, J.; et al. Association of insulin resistance and type 2 diabetes with gut microbial diversity: A microbiome-wide analysis from population studies. *JAMA Netw. Open* **2021**, *4*, e2118811. [CrossRef]
22. Lu, T.J.; Chiou, W.C.; Huang, H.C.; Pan, H.C.; Sun, C.Y.; Way, T.D.; Huang, C. Modulation of gut microbiota by crude gac aril polysaccharides ameliorates diet-induced obesity and metabolic disorders. *Int. J. Biol. Macromol.* **2024**, *273*, 133164. [CrossRef] [PubMed]
23. Zheng, X.; Zhang, Z.; Shan, T.; Zhao, M.; Lu, H.; Zhang, L.; Liang, X. Study on the mechanism of Bifidobacterium animalis subsp. lactis F1-3-2 regulating bile acid metabolism through TMA-TMAO pathway to improve atherosclerosis. *Probiotics Antimicrob. Proteins* **2024**, *17*, 4851–4866. [CrossRef] [PubMed]
24. Guo, G.; Wu, Y.; Liu, Y.; Wang, Z.; Xu, G.; Wang, X.; Liang, F.; Lai, W.; Xiao, X.; Zhu, Q.; et al. Exploring the causal effects of the gut microbiome on serum lipid levels: A two-sample Mendelian randomization analysis. *Front. Microbiol.* **2023**, *14*, 1113334. [CrossRef] [PubMed]
25. Lee, S.H.; You, H.S.; Kang, H.G.; Kang, S.S.; Hyun, S.H. Association between altered blood parameters and gut microbiota after synbiotic intake in healthy, elderly Korean women. *Nutrients* **2020**, *12*, 3112. [CrossRef]
26. Ho, J.; Nicolucci, A.C.; Virtanen, H.; Schick, A.; Meddings, J.; Reimer, R.A.; Huang, C. Effect of prebiotic on microbiota, intestinal permeability, and glycemic control in children with type 1 diabetes. *J. Clin. Endocrinol. Metab.* **2019**, *104*, 4427–4440. [CrossRef]
27. Hou, K.; Wu, Z.X.; Chen, X.Y.; Wang, J.Q.; Zhang, D.; Xiao, C.; Zhu, D.; Koya, J.B.; Wei, L.; Li, J.; et al. Microbiota in health and diseases. *Signal Transduct. Target. Ther.* **2022**, *7*, 135. [CrossRef]
28. Ohkawara, S.; Furuya, H.; Nagashima, K.; Asanuma, N.; Hino, T. Effect of oral administration of Butyrivibrio fibrisolvens MDT-1 on experimental enterocolitis in mice. *Clin. Vaccine Immunol.* **2006**, *13*, 1231–1236. [CrossRef]
29. Zong, X.; Zhang, H.; Zhu, L.; Deehan, E.C.; Fu, J.; Wang, Y.; Jin, M. Auricularia auricula polysaccharides attenuate obesity in mice through gut commensal Papillibacter cinnamivorans. *J. Adv. Res.* **2023**, *52*, 203–218. [CrossRef]
30. Cao, Z.; Yang, J.; Mai, H.; Hong, T.; Chen, X.; Feng, D. Dietary curcumin prevents hypercholesterolemia by inhibiting the transcriptional activity of SREBP-2 and HNF1α and reducing intestinal and hepatic NPC1L1 expression in high-fat diet-fed hamsters. *Nutr. Metab.* **2025**, *22*, 128. [CrossRef]
31. Wang, T.; Lan, Q.; Deng, H.; Han, W.; Zhang, R.; Zhong, J. Interactions between gut microbiota and cardiovascular drugs: Effects on drug therapeutic effect and side effect. *Front. Cardiovasc. Med.* **2025**, *12*, 1570008. [CrossRef] [PubMed]
32. Sivri, D.; Akdevelioğlu, Y. Effect of fatty acids on glucose metabolism and type 2 diabetes. *Nutr. Rev.* **2025**, *83*, 897–907. [CrossRef] [PubMed]
33. Milena, E.; Maurizio, M. Exploring the cardiovascular benefits of extra virgin olive oil: Insights into mechanisms and therapeutic potential. *Biomolecules* **2025**, *15*, 284. [CrossRef] [PubMed]
34. De Filippo, C.; Costa, A.; Becagli, M.V.; Monroy, M.M.; Provensi, G.; Passani, M.B. Gut microbiota and oleoylethanolamide in the regulation of intestinal homeostasis. *Front. Endocrinol.* **2023**, *14*, 1135157. [CrossRef]
35. Kopp, L.; Seethaler, B.; Neumann, U.; Bischoff, S.C. Oral intake of the microalgae *Nannochloropsis oceanica*, *Chlorella vulgaris*, or *Phaeodactylum tricornutum* improves metabolic conditions in hypercaloric-fed mice. *J. Funct. Foods* **2024**, *121*, 106429. [CrossRef]
36. Huang, H.; Liao, D.; Pu, R.; Cui, Y. Quantifying the effects of spirulina supplementation on plasma lipid and glucose concentrations, body weight, and blood pressure. *Diabetes Metab. Syndr. Obes.* **2018**, *11*, 729–742. [CrossRef]
37. Tredici, M.R.; Rodolfi, L.; Biondi, N.; Bassi, N.; Sampietro, G. Techno-economic analysis of microalgal biomass production in a 1-ha Green Wall Panel (GWP®) plant. *Algal Res.* **2016**, *19*, 253–263. [CrossRef]
38. Guillard, R.R.L.; Ryther, J.H. Studies of marine planktonic diatoms. I. Cyclotella nana Hustedt and Detonula confervacea Cleve. *Can. J. Microbiol.* **1962**, *8*, 229–239. [CrossRef]
39. Dubois, M.; Gilles, K.A.; Hamilton, J.K.; Rebers, P.; Smith, F. Colorimetric method for determination of sugars and related substances. *Anal. Chem.* **1956**, *28*, 350–356. [CrossRef]
40. Marsh, J.B.; Weinstein, D.B. Simple charring method for determination of lipids. *J. Lipid Res.* **1966**, *7*, 574–576. [CrossRef]
41. Abiusi, F.; Sampietro, G.; Marturano, G.; Biondi, N.; Rodolfi, L.; D'Ottavio, M.; Tredici, M.R. Growth, photosynthetic efficiency, and biochemical composition of *Tetraselmis suecica* F&M-M33 grown with LEDs of different colors. *Biotechnol. Bioeng.* **2014**, *111*, 956–964. [CrossRef] [PubMed]

42. Kim, S.M.; Kang, S.W.; Kwon, O.N.; Chung, D.; Pan, C.H. Fucoxanthin as a major carotenoid in Isochrysis aff. galbana: Characterization of extraction for commercial application. *J. Korean Soc. Appl. Biol. Chem.* **2012**, *55*, 477–483. [CrossRef]
43. Kraus, D.; Yang, Q.; Kahn, B.B. Lipid extraction from mouse feces. *Bio-Protoc.* **2015**, *5*, e1375. [CrossRef] [PubMed]
44. Martin, M. Cutadapt removes adapter sequences from high-throughput sequencing reads. *EMBnet. J.* **2011**, *17*, 10–12. [CrossRef]
45. Callahan, B.J.; McMurdie, P.J.; Rosen, M.J.; Han, A.W.; Johnson, A.J.A.; Holmes, S.P. Dada2: High-resolution sample inference from Illumina amplicon data. *Nat. Methods* **2016**, *13*, 581–583. [CrossRef]
46. Wright, E.S. Using DECIPHER v2.0 to analyze big biological sequence data in R. *R J.* **2016**, *8*, 352–359. [CrossRef]
47. R Core Team. *R: A Language and Environment for Statistical Computing*; R Foundation for Statistical Computing: Vienna, Austria, 2023. Available online: https://www.R-project.org/ (accessed on 1 September 2024).
48. Oksanen, J.; Simpson, G.; Blanchet, F.; Kindt, R.; Legendre, P.; Minchin, P.; O'Hara, R.; Solymos, P.; Stevens, M.; Szoecs, E.; et al. *vegan: Community Ecology Package*. 2025. Available online: https://cran.r-project.org/web/packages/vegan/index.html (accessed on 18 February 2026).
49. Martinez, A.P. pairwiseAdonis: Pairwise Multilevel Comparison Using Adonis. R Package Version 0.4.1. 2017. Available online: https://github.com/pmartinezarbizu/pairwiseAdonis (accessed on 12 July 2024).
50. McMurdie, P.J.; Holmes, S. phyloseq: An R package for reproducible interactive analysis and graphics of microbiome census data. *PLoS ONE* **2013**, *8*, e61217. [CrossRef]
51. Shuangbin, X.; Li, Z.; Wenli, T.; Qianwen, W.; Zehan, D.; Lang, Z.; Tingze, F.; Meijun, C.; Tianzhi, W.; Erqiang, H.; et al. MicrobiotaProcess: A comprehensive R package for deep mining microbiome. *Innovation* **2023**, *4*, 100388. [CrossRef]
52. Harrell, F., Jr. Hmisc: Harrell Miscellaneous; R Package Version 5.2-3. 2025. Available online: https://CRAN.R-project.org/package=Hmisc (accessed on 14 March 2025).
53. Csardi, G.; Nepusz, T. The igraph software. *Complex Syst.* **2006**, *1695*, 1–9.
54. Pedersen, T. ggraph: An Implementation of Grammar of Graphics for Graphs and Networks. R Package Version 2.2.2. 2025. Available online: https://CRAN.R-project.org/package=ggraph (accessed on 1 November 2025).
55. Bartolucci, G.; Pallecchi, M.; Menicatti, M.; Moracci, L.; Pucciarelli, S.; Agostini, M.; Crotti, S. A method for assessing plasma free fatty acids from C2 to C18 and its application for the early detection of colorectal cancer. *J. Pharm. Biomed. Anal.* **2022**, *215*, 114762. [CrossRef]

Disclaimer/Publisher's Note: The statements, opinions and data contained in all publications are solely those of the individual author(s) and contributor(s) and not of MDPI and/or the editor(s). MDPI and/or the editor(s) disclaim responsibility for any injury to people or property resulting from any ideas, methods, instructions or products referred to in the content.